Infrared and Raman Spectra of Inorganic and Coordination Compounds

Part B: Applications in Coordination, Organometallic, and Bioinorganic Chemistry

Sixth Edition

Kazuo Nakamoto

Wehr Professor Emeritus of Chemistry
Marquette University

WILEY

*Infrared and Raman
Spectra of Inorganic and
Coordination Compounds*

Infrared and Raman Spectra of Inorganic and Coordination Compounds

Part B: Applications in Coordination, Organometallic, and Bioinorganic Chemistry

Sixth Edition

Kazuo Nakamoto

Wehr Professor Emeritus of Chemistry
Marquette University

WILEY

Contents

Preface to the Sixth Edition

Since the fifth edition was published in 1996, a number of new developments have been made in the field of infrared and Raman spectra of inorganic and coordination compounds. The sixth edition is intended to emphasize new important developments as well as to catch up with the ever-increasing new literature. Major changes are described below.

Part A. Chapter 1 ("Theory of Normal Vibrations") includes two new sections. Section 1.24 explains the procedure for calculating vibrational frequencies on the basis of density functional theory (DFT). The DFT method is currently used almost routinely to determine molecular structures and to calculate vibrational parameters. Section 1.26 describes new developments in matrix cocondensation techniques. More recently, a large number of novel inorganic and coordination compounds have been prepared by using this technique, and their structures have been determined and vibrational assignments have been made on the basis of results of DFT calculations. Chapter 2 ("Applications in Inorganic Chemistry") has been updated extensively, resulting in a total number of references of over 1800. In particular, sections on triangular X_3- and tetrahedral X_4-type molecules have been added as Secs. 2.2 and 2.5, respectively. In Sec. 2.8, the rotational–vibrational spectrum of the octahedral UF_6 molecule is shown to demonstrate how an extremely small metal isotope shift by $^{235}U/^{238}U$ substitution (only $0.6040\,cm^{-1}$) can be measured. Section 2.14 ("Compounds of Carbon") has been expanded to show significant applications of vibrational spectroscopy to the structural determination of fullerenes, endohedral fullerenes, and carbon nanotubes. Vibrational data on a number of novel inorganic compounds prepared most recently have been added throughout Chapter 2.

Part B. Chapter 1 ("Applications in Coordination Chemistry") contains two new Sections: Sec. 1.6 ("Metallochlorins, Chlorophylls, and Metallophthalocyanines")

and Sec. 1.19 ("Complexes of Carbon Dioxide"). The total number of references has approached 1700 because of substantial expansion of other sections such as Secs. 1.5, 1.18, 1.20, 1.22, and 1.28. Chapter 2 ("Applications in Organometallic Chemistry") includes new types of organometallic compounds obtained by matrix cocondensation techniques (Sec. 2.1). In Chapter 3 ("Applications in Bioinorganic Chemistry"), a new section (Sec. 3.4) has been added, and several sections such as Secs. 3.3, 3.7, and 3.9 have been expanded to include many important new developments.

I would like to express my sincere thanks to all who helped me in preparing this edition. Special thanks go to Prof. J. R. Kincaid (Marquette University), Prof. R. S. Czernuszewicz (University of Houston), and Dr. T. Kitagawa (Institute for Molecular Science, Okazaki, Japan) for their help in writing new sections of Chapter 3 of Part B. My thanks also go to all the authors and publishers who gave me permission to reproduce their figures in this and previous editions.

Finally, I would like to thank the staff of John Raynor Science Library of Marquette University for their help in collecting new references.

Milwaukee, Wisconsin   KAZUO NAKAMOTO
March 2008

Abbreviations

Several different groups of acronyms and other abbreviations are used:

1. IR, infrared; R, Raman; RR, resonance Raman; p, polarized; dp, depolarized; ap, anomalous polarization; ia, inactive.
2. ν, stretching; δ, in-plane bending or deformation; ρ_w, wagging; ρ_r, rocking; ρ_t, twisting; π, out-of-plane bending. Subscripts, a, s, and d denote antisymmetric, symmetric, and degenerate modes, respectively. Approximate normal modes of vibration corresponding to these vibrations are given in Figs. 1.25 and 1.26.
3. DFT, density functional theory; NCA, normal coordinate analysis; GVF, generalized valence force field; UBF, Urey–Bradley force field.
4. M, metal; L, ligand; X, halogen; R, alkyl group.
5. g, gas; l, liquid; s, solid; m or mat, matrix; sol'n or sl, solution; (gr) or (ex), ground or excited state.
6. Me, methyl; Et, ethyl; Pr, propyl; Bu, butyl; Ph, phenyl; Cp, cyclopentadienyl; OAc^-, acetate ion; py, pyridine; pic, pycoline; en, ethylenediamine. Abbreviations of other ligands are given when they appear in the text.

In the tables of observed frequencies, values in parentheses are calculated or estimated values unless otherwise stated.

Chapter **1**

Applications in Coordination Chemistry

1.1. AMMINE, AMIDO, AND RELATED COMPLEXES

1.1.1. Ammine (NH$_3$) Complexes

Vibrational spectra of metal ammine complexes have been studied extensively, and these are reviewed by Schmidt and Müller [1]. Figure 1.1 shows the infrared spectra of typical hexammine complexes in the high-frequency region. To assign these NH$_3$ group vibrations, it is convenient to use the six normal modes of vibration of a simple 1:1 (metal/ligand) complex model such as that shown in Fig. 1.2. Table 1.1 lists the infrared frequencies and band assignments of hexammine complexes. It is seen that the antisymmetric and symmetric NH$_3$ stretching, NH$_3$ degenerate deformation, NH$_3$ symmetric deformation, and NH$_3$ rocking vibrations appear in the regions of 3400–3000, 1650–1550, 1370–1000, and 950–590 cm^{-1}, respectively. These assignments have been confirmed by NH$_3$/ND$_3$ and NH$_3$/^{15}NH$_3$ isotope shifts.

   The NH$_3$ stretching frequencies of the complexes are lower than those of the free NH$_3$ molecule for two reasons. One is the effect of coordination. On coordination, the N−H bond is weakened and the NH$_3$ stretching frequencies are lowered. The stronger the M−N bond, the weaker is the N−H bond and the lower are the NH$_3$ stretching frequencies if other conditions are equal. Thus the NH$_3$ stretching frequencies may be used as a rough measure of the M−N bond strength. The other reason is the effect of the counterion. The NH$_3$ stretching frequencies of the chloride
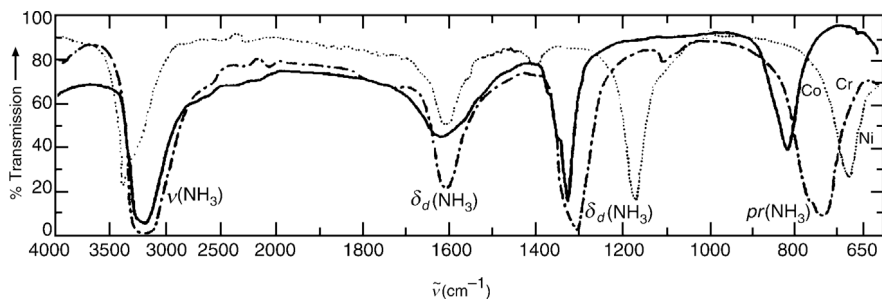
Fig. 1.1. *Infrared spectra of hexammine complexes: [Co(NH₃)₆]Cl₃ (solid line), [Cr(NH₃)₆]Cl₃ (dotted–dashed line), and [Ni(NH₃)₆]Cl₂ (dotted line).*

are much lower than those of the perchlorate, for example. This is attributed to the weakening of the N−H bond, due to the formation of the N−H···Cl-type hydrogen bond in the former.

The effects of coordination and hydrogen bonding mentioned above shift the NH₃ deformation and rocking modes to higher frequencies. Among them, the NH₃ rocking mode is most sensitive, and the degenerate deformation is least sensitive, to these effects. Thus the NH₃ rocking frequency is often used to compare the strength of the M−N bond in a series of complexes of the same type and anion. As will be shown in
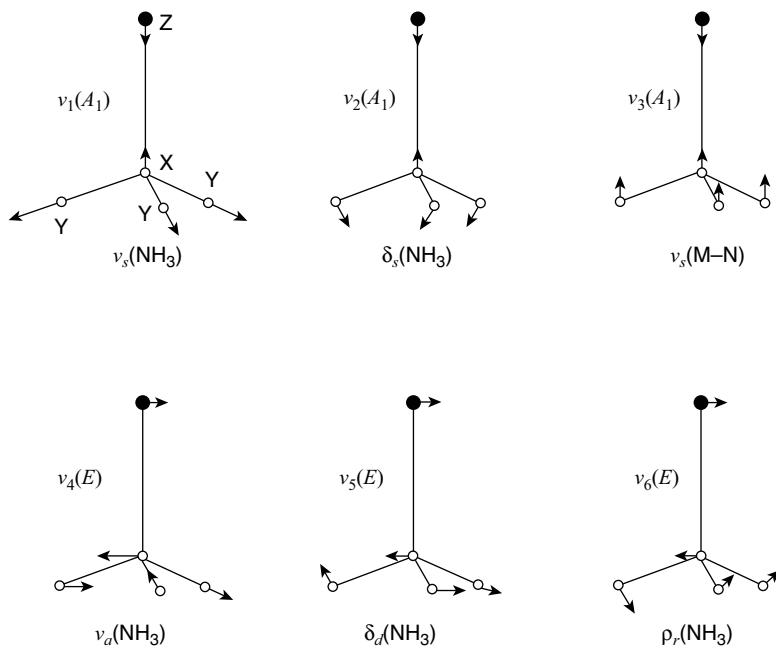
Fig. 1.2. *Normal modes of vibration of tetrahedral ZXY₃ molecules. (The band assignment is given for an M−NH₃ group.)*

TABLE 1.1. Infrared Frequencies of Octahedral Hexammine Complexes (cm^{-1})[a]

Complex	$\nu_a(NH_3)$	$\nu_s(NH_3)$	$\delta_a(HNH)$	$\delta_s(HNH)$	$\rho_r(NH_3)$	$\nu(MN)$ IR	$\nu(MN)$ Raman	$\delta(NMN)$	Ref.
$[Mg(NH_3)_6]Cl_2$	3353	3210	1603	1170	660	363	335 (A_{1g}) 243 (E_g)	198	2
$[Cr(NH_3)_6]Cl_3$	3257	3185 3130	1630	1307	748	495 473 456	465 (A_{1g}) 412 (E_g)	—	3
$[^{50}Cr(NH_3)_6](NO_3)_3$	3310	3250 3190	1627	1290	770	471	—	270	4
$[Mn(NH_3)_6]Cl_2$	3340	3160	1608	1146	592	302	330 (A_{1g})	165	1,5
$[Fe(NH_3)_6]Cl_2$	3335	3175	1596	1156	633	315	—	170	1,5
$[Ru(NH_3)_6]Cl_2$	3315	3210	1612	1220	763	409	—	—	6
$[Ru(NH_3)_6]Cl_3$	3077		1618	1368 1342	788	463	500 (A_{1g}) 475 (E_g)	283 263	7
$[Os(NH_3)_6]OsBr_6$	3125	3250	1595	1339	818	452	—	256	7
$[Co(NH_3)_6]Cl_2$	3330	3160	1602	1163	654	325	357 (A_{1g}) 255 (E_g)	92	5
$[Co(NH_3)_6]Cl_3$	3240		1619	1329	831	498 477 449	500 (A_{1g}) 445 (E_g)	331	8~10
$[Co(ND_3)_6]Cl_3$	2440	2300	1165	1020	667	462 442 415	—	294	4
$[Rh(NH_3)_6]Cl_3$	3200		1618	1352	845	472	515 (A_{1g}) 480 (E_g)	302	7,10
$[Ir(NH_3)_6]Cl_3$	3155		1587	1350 1323	857	475	527 (A_{1g}) 500 (E_g)	279 264	7,10
$[^{58}Ni(NH_3)_6]Cl_2$	3345	3190	1607	1176	685	335	370 (A_{1g}) 265 (E_g)	217	8,11
$[Zn(NH_3)_6]Cl_2$	3350	3220	1596	1145	645	300	—	—	1
$[Cd(NH_3)_6]Cl_2$	—	—	1585	1091	613	298	342 (A_{1g})	—	5
$[Pt(NH_3)_6]Cl_4$	3150	3050	1565	1370	950	530 516	569 (A_{1g}) 545 (E_g)	318	12,13

[a]All infrared frequencies are those of the F_{1u} species.

the next subsection, a simple 1 : 1 complex such as that shown in Fig. 1.2 has been prepared in inert gas matrices [30].

To assign the skeletal modes such as the MN stretching and NMN bending modes, it is necessary to consider the normal modes of the octahedral MN_6 skeleton ($\mathbf{O}_h$ symmetry). The MN stretching mode in the low-frequency region is of particular interest since it provides direct information about the structure of the MN skeleton and the strength of the M—N bond. The octahedral MN_6 skeleton exhibits two $v(M-N)$ (A_{1g} and E_g) in Raman and one $v(M-N)$ (F_{1u}) in infrared spectra (see Sec. 2.8 of Part A). Most of these vibrations have been assigned on the basis of observed isotope shifts (including metal isotopes, NH_3/ND_3 and $NH_3/^{15}NH_3$) and normal coordinate calculations. Although the assignment of the $v(Co-N)$ in the infrared spectrum of [Co$(NH_3)_6]Cl_3$ had been controversial, Schmidt and Müller [4] confirmed the assignments that the three weak bands at 498, 477, and 449 cm^{-1} are the split components of the triply degenerate F_{1u} mode (Fig. 1.4). The intensity of the MN stretching mode in the infrared increases as the M—N bond becomes more ionic and as the MN stretching frequency becomes lower. Relative to the Co(III)—N bond of the $[Co(NH_3)_6]^{3+}$ ion, the Co(II)—N bond of the $[Co(NH_3)_6]^{2+}$ ion is more ionic, and its stretching frequency is much lower (325 cm^{-1}). This may be responsible for the strong appearance of the Co(II)—N stretching band in the infrared. As listed in Table 1.1, two Raman-active MN stretching modes (A_{1g} and E_g) are observed for the octahedral hexammine salts. In general, $v(A_{1g})$ is higher than $v(E_g)$. However, the relative position of $v(F_{1u})$ with respect to these two vibrations changes from one compound to another. Another obvious trend in $v(MN)$ is $v(M^{4+}-N) > v(M^{3+}-N) > v(M^{2+}-N)$. This holds for all symmetry species. Table 1.1 shows that the NH_3 rocking frequency also follows the same trend as above.

Normal coordinate analyses on metal ammine complexes have been carried out by many investigators. Among them, Nakagawa, Shimanouchi, and coworkers [13] have undertaken the most comprehensive study, using the UBF (Urey–Bradley Force) field. The MN stretching force constants of the hexammine complexes follow this order:

$$\text{Pt(IV)} \gg \text{Co(III)} > \text{Cr(III)} > \text{Ni(II)} \approx \text{Co(II)}$$
$$2.13 \qquad 1.05 \qquad 0.94 \qquad 0.34 \qquad 0.33 \;\; \text{mdyn}/\text{Å}$$

Acevedo and coworkers carried out normal coordinate calculations on the [Cr$(NH_3)_6]^{3+}$ and $[Ni(NH_3)_6]^{2+}$ ions [14,15]. On the other hand, Schmidt and Müller [4,5] and other workers [8] calculated the GVF (generalized valence Force) constants of a number of ammine complexes by using the point mass model (where the NH_3 ligand is regarded as a single atom having the mass of NH_3), and refined their values with isotope shift data (H/D, $^{14}N/^{15}N$, and metal isotopes). For the hexammine series, they obtained the following order:

$$\text{Pt}^{4+} > \text{Ir}^{3+} > \text{Os}^{3+} > \text{Rh}^{3+} > \text{Ru}^{3+} > \text{Co}^{3+} >$$
$$2.75 \quad 2.28 \quad 2.13 \quad 2.10 \quad 2.01 \quad 1.86$$

$$\text{Cr}^{3+} > \text{Ni}^{2+} > \text{Co}^{2+} > \text{Fe}^{2+} \sim \text{Cd}^{2+} > \text{Zn}^{2+} > \text{Mn}^{2+}$$
$$1.66 \quad 0.85 \quad 0.80 \quad 0.73 \quad 0.69 \quad 0.67 \;\; \text{mdyn}/\text{Å}$$

TABLE 1.2. Infrared Frequencies of Other Ammine Complexes (cm^{-1})

Complex	$\nu_a(NH_3)$	$\nu_s(NH_3)$	$\delta_a(HNH)$	$\delta_s(HNH)$	$\rho_r(NH_3)$	$\nu(MN)$ IR	Raman	$\delta(NMN)$	Ref.
Tetrahedral									
[Co(NH$_3$)$_4$](ReO$_4$)$_2$	3340	3260	1610	1240	693	430	405 (A_1)	195	16
[^{64}Zn(NH$_3$)$_4$]I$_2$	3275	3150	1596	1253	685	—	432 (A_1)	156	17,18
	3233			1239			412 (F_2)		
[Cd(NH$_3$)$_4$](ReO$_4$)$_2$	3354	3267	1617	1176	670	370	—	166	1,19
								160	
Square-planar									
[^{104}Pd(NH$_3$)$_4$]Cl$_2$·H$_2$O	3270	3170	1630	1279	849	495	502 (A_{1g})	325	4,20,21
					802		482 (B_{1g})	300	
[Pt(NH$_3$)$_4$]Cl$_2$	3236	3156	1563	1325	842	510	543 (A_{1g})	301	13,22,21
							522 (B_{1g})		
[Cu(NH$_3$)$_4$]So$_4$·H$_2$O	3327	3169	1669	1300	735	426	420 (A_{1g})	256	4,23
	3253		1639	1283			375 (B_{1g})	227	
[Au(NH$_3$)$_4$](NO$_3$)$_3$	3490	3105	1571	1331	936	555	566	327	24
	3220				914		544	307	
								272	
Linear									
[Ag(NH$_3$)$_2$]So$_4$	3320	3150	1642	1236	740	476	372 (A_1)	221	25,26
	3230		1626	1222	703	400		211	27
[Hg(NH$_3$)$_2$]Cl$_2$	3265	3197	1605	1268	719	513	412	—	

For a series of divalent metals, this order is parallel to the Irving–Williams series ($Mn^{2+} < Fe^{2+} < Co^{2+} < Ni^{2+} < Cu^{2+} > Zn^{2+}$). Schmidt and Müller [1] discussed the relationship between the MN stretching force constant and the stability constant or the bond energy.

Table 1.2 lists the observed infrared frequencies and band assignments of tetrahedral, square–planar, and linear metal ammine complexes. The Raman-active MN stretching frequencies are also included in Table 1.2. Normal coordinate analyses have been made by Nakagawa et al. [13] by using the UBF field; the following values were obtained for the MN stretching force constants:

$$Hg^{2+} > Pt^{2+} > Pd^{2+} > Cu^{2+}$$
$$2.05 \quad 1.92 \quad 1.71 \quad 0.84 \quad mdyn/\mathring{A}$$

Normal coordinate calculations have also been made by Tellez [28] on the tetrahedral $[Zn(NH_3)_4]^{2+}$ and $[Cd(NH_3)_4]^{2+}$ ions. Using the GVF field and the point mass approximation, Schmidt and Müller [5] obtained the following values:

$$Pt^{2+} > Pt^{2+} \gg Co^{2+} \sim Zn^{2+} \sim Cu^{2+} > Cd^{2+}$$
$$2.54 \quad 2.15 \quad 1.44 \quad 1.43 \quad 1.42 \quad 1.24 \quad mdyn/\mathring{A}$$

As stated above, NH_3 frequencies of ammine complexes are determined by the strength of the M−N bond as well as the strength of the N−H$\cdots$X hydrogen bond. The order of this synergetic effect has been studied for $[M(NH_3)_6]X_2$-type complexes [29].

1.1.2. Ammine Complexes in Inert Gas Matrices

Infrared spectra of cocondensation products of alkali halide (MX) vapors with NH_3 diluted in argon were measured by Ault [34]. In the case of KCl, for example, the bands at 3365, 3177, and 1103 cm^{-1} have been assigned to the $v_a(NH_3)$, $v_s(NH_3)$, $\delta_s(HNH)$, respectively, of the 1 : 1 ion pair of type I shown below:
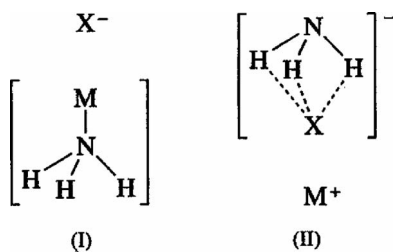

The type II structure was ruled out because of the following reasons: (1), the $\delta_s(HNH)$ frequency should be sensitive to the metal ion in (I) and to the anion in (II) [the fact that it shows relatively large shifts by changing the metal ion, but almost no shifts by changing the anion, supports (I)]; and (2) the $v_a(NH_3)$ and $v_s(NH_3)$ in (II) are expected to be highly sensitive to the anion, owing to formation of the N−H$\cdots$X hydrogen bonds; this is not the case in (I). The fact that they show only small shifts in going from CsCl to CsI supports (I). Further supports for structure (I) are given by the appearance of the $\rho_r(NH_3)$ and $v(M-N)$ at 458 and 232 cm^{-1} (KCl), respectively. These frequencies are much lower than those of transition metal complexes discussed earlier, because their M−N bonds are much weaker (more ionic).

Süzer and Andrews [31] studied the IR spectra of cocondensation products of alkali metal (M) vapors with NH_3/Ar. They assigned the following bands:

	Li	Na	K	Cs	
$v_s(NH_3)$	3277	3294	3292	3287	(all in cm^{-1})
$\delta_s(NH_3)$	1133	1079	1064	1049	

to the 1 : 1 adduct of $\mathbf{C}_{3v}$ symmetry which is similar to that of the $M(NH_3)^+$ cation discussed earlier. The M−NH_3 bonding has been attributed to a small charge transfer from NH_3 to M in the case of Li and Na, and to a reverse charge transfer in the case of K and Cs. At high concentrations of M and NH_3, large aggregates of undefined stoichiometries were formed. Similar work including Fe and Cu was carried out by Szczepanski et al. [32] Loutellier et al. [33] have made the most extensive IR study on the Li(K)/NH_3/Ar system. By varying the concentrations and relative ratios of M/NH_3 in a wide range, they were able to observe bands characteristic of the 1 : 1, 1 : 2, . . ., 1 : n,
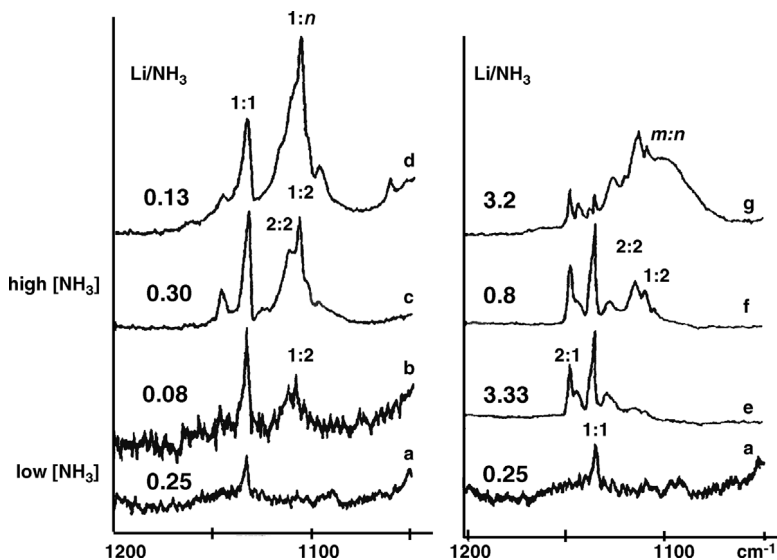
Fig. 1.3. IR spectra (1200–1050 cm^{-1}) of cocondensation products of Li atoms with NH$_3$ molecules in Ar matrices. Left column: (a) Li/NH$_3$/Ar = 0.1/0.4/1000, (b) 0.1/1.2/1000, (c) 3/10/1000, and (d) 2.5/20/1000. Right column: (a) Li/NH$_3$/Ar = 0.1/0.4/1000, (e) 2/0.6/1000, (f) 2/2.5/1000, and (g) 8/2.5/1000 [33].

and $2:1, 3:1 \cdots m:1$ adducts. As an example, Fig. 1.3 shows the IR spectra of the Li/ NH$_3$/Ar system in the δ_s(NH$_3$) region. The molar ratios (Li/NH$_3$) and the peaks characteristic of each species are indicated in the figure. In general, the $1:1$ adduct is formed when the concentrations of Li and NH$_3$ are close. If the concentration of NH$_3$ is high relative to Li, the $1:n$ ($n=2,3,4,\ldots$) adducts are formed. On the other hand, the $m:1$ ($m=2,3,4\ldots$) adducts result when the concentration of Li is high relative to NH$_3$. For the $1:1$ adduct of Li, the bands at 381 and 320 cm^{-1} have been assigned to the ρ_r(NH$_3$) and v(Li—N), respectively. The Li—N stretching force constant was found to be 0.3 mdyn/Å.

Photolysis of ammine complexes in inert gas matrices has been used to produce a number of new species. For example, Ault [34] obtained Cl$_2$V(O)NH$_2$ by the reaction

$$\text{OVCl}_3 + \text{NH}_3 \xrightarrow{\text{in Ar}} \text{OVCl}_3 - \text{NH}_3 \xrightarrow{h\nu} \text{Cl}_2\text{V(O)NH}_2 + \text{HCl}$$
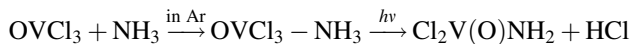
and its infrared spectrum was assigned by isotopic substitution (H/D and ^{14}N/^{15}N) and DFT calculations. Similar reactions have been utilized to prepare HSiNH$_2$ [35] and HMNH$_2$(M = Al,Ga, In) [36].

1.1.3. Halogenoammine Complexes

If the NH$_3$ groups of a hexammine complex are partly replaced by other groups, the degenerate vibrations are split because of lowering of symmetry, and new

TABLE 1.3. Skeletal Vibrations of Pentammine and *trans*-Tetrammine Co (III) Complex (cm^{-1}) [37,38]

Complex	ν(CoN)	ν(CoX)	Skeletal Bending
Pentammine (**C**$_{4v}$)			
[Co(NH$_3$)$_5$F]$^{2+}$			
A_1	480, 438	343	308
E	498	—	345, 290, 219
[Co(NH$_3$)$_5$Cl]$^{2+}$			
A_1	476, 416	272	310
E	498	—	292, 287, 188
[Co(NH$_3$)$_5$Br]$^{2+}$			
A_1	475, 410	215	287
E	497	—	290, 263, 146
[Co(NH$_3$)$_5$I]$^{2+}$			
A_1	473, 406	168	271
E	498	—	290, 259, 132
trans-Tetrammine (**D**$_{4h}$)			
[Co(NH$_3$)$_4$Cl$_2$]$^+$			
A_{2u}	—	353	186
E_u	501	—	290, 167
[Co(NH$_3$)$_4$Br$_2$]$^+$			
A_{2u}	—	317	227
E_u	497	—	280, 120

bands belonging to other groups appear. Here we discuss only halogenoammine complexes. The infrared spectra of [Co(NH$_3$)$_5$X]$^{2+}$- and *trans*-[Co(NH$_3$)$_4$X$_2$]$^+$-type complexes have been studied by Nakagawa and Shimanouchi [37,38]. Table 1.3 lists the observed frequencies and band assignments obtained by these workers. The infrared spectra of some of these complexes in the CoN stretching region are shown in Fig. 1.4. Normal coordinate analyses on these complexes [37] have yielded the following UBF stretching force constants (mdyn/Å): K(Co−N), 1.05; K(Co−F), 0.99; K(Co−Cl), 0.91; K(Co−Br), 1.03; and K(Co−I), 0.62.

Using the GVF force field, Chen et al. [39,40] also carried out normal coordinate analysis on [M(NH$_3$)$_5$X]-type complexes (M = Co, Cr; X = NH$_3$, Cl, H$_2$O, OH, etc.) to obtain the ν(M−N) and ν(M−X) force constants.

Raman spectra of some chloroammine Co(III) complexes have been assigned [41]. In the series of the [Cr(NH$_3$)$_5$X]$^{2+}$ ions, the ν(Cr−N) are in the 475–400 cm^{-1} region, and the ν(Cr−X) are at 540, 302, 264, and 184 cm^{-1}, respectively, for X = F, Cl, Br, and I [42]. For more information on halogenoammine complexes of Cr(III), see Ref. [43]. Detailed vibrational assignments are available for halogenoammine complexes of Os(III) [44] and of Ru(III), Rh(III), Os(III), and Ir(III) [45].

In regard to M(NH$_3$)$_4$X$_2$- and M(NH$_3$)$_3$X$_3$-type complexes, the main interest has been the distinction of stereoisomers by vibrational spectroscopy. As shown in

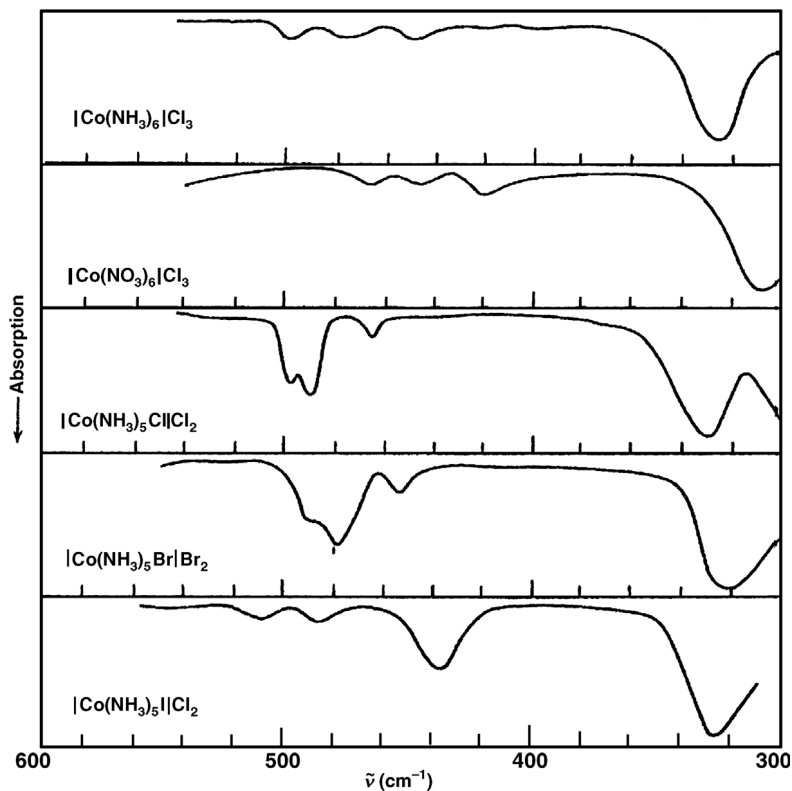**Fig. 1.4.** Infrared spectra (600–300 cm^{-1}) of Co(III) halogenoammine complexes.

Appendix V of Part A, *trans*-MN$_4$X$_2$ ($\mathbf{D}_{4h}$) exhibits one MN stretching (E_u) and one MX stretching (A_{2u}), while *cis*-MN$_4$X$_2$ ($\mathbf{C}_{2v}$) shows four MN stretching (two A_1, B_1, and B_2) and two MX stretching (A_1 and B_1) vibrations in the infrared. For *mer*-MN$_3$X$_3$ ($\mathbf{C}_{2v}$), three MN stretching and three MX stretching vibrations are infrared-active, whereas only two MN stretching and two MX stretching vibrations are infrared-active for *fac*-MN$_3$X$_3$ ($\mathbf{C}_{3v}$). Nolan and James [12] have measured and assigned the Raman spectra of a series of [Pt(NH$_3$)$_n$Cl$_{6-n}$]$^{(n-2)+}$-type complexes. Li et al. [46] carried out normal coordinate analysis on *cis*-Pt(NH$_3$)$_2$Cl$_4$.

Vibrational spectra of the planar M(NH$_3$)$_2$X$_2$-type complexes [M = Pt(II), Pd(II)] have been studied by many investigators. Table 1.4 summarizes the observed frequencies and band assignments of their skeletal vibrations, including those of "*cis*-platin"—the well-known anticancer drug. Figure 1.5 shows the infrared spectra of *cis*- and *trans*-[Pd(NH$_3$)$_2$Cl$_2$] obtained by Layton et al. [51]. As expected, both the PdN and PdCl stretching bands split into two in the *cis*-isomer. Durig et al. [52] found that the PdN stretching frequencies range from 528 to 436 cm^{-1}, depending on the

TABLE 1.4. Skeletal Frequencies of Square–Planar M(NH₃)₂X₂-Type Complexes (cm⁻¹)ᵃ

Complex	ν(MN)	ν(MX)	Bending	Ref.
trans-[Pd(NH₃)₂Cl₂]				
IR	496	333	245, 222, 162, 137	47,21
R	492	295	224	
cis-[Pd(NH₃)₂Cl₂]				
IR	495, 476	327, 306	245, 218, 160, 135	47
trans-[Pd(NH₃)₂Br₂]				
IR	490	—	220, 220, 122, 101	47
R	483	182	172	21
cis-[Pd(NH₃)₂Br₂]				
IR	480, 460	258	225, 225, 120, 100	47
trans-[Pd(NH₃)₂I₂]				
IR	480	191	263, 218, 109	47
trans-[Pt(NH₃)₂Cl₂]				
IR	572	365	220, 195	48,49
R	538	334	—	21,48
cis-[Pt(NH₃)₂Cl₂]ᵇ				
IR	510	330, 323	250, 198, 155, 123	49
R	507	253	160	21
trans-[Pt(NH₃)₂Br₂]				
IR	504	260	230	48,49
R	535	206	—	48
trans-[Pt(NH₃)₂I₂]				
R	532	153	—	48

ᵃFor band assignments, see also Refs. 13 and 50.
ᵇSee Sec. 3.9.1.

nature of other ligands in the complex. In general, the PtN stretching band shifts to a lower frequency as a ligand of stronger *trans* influence is introduced in the position *trans* to the Pt−N bond. Using infrared spectroscopy, Durig and Mitchell [53] studied the isomerization of *cis*-[Pd(NH₃)₂X₂] to its *trans*-isomer.

Other studies on halogenoammine complexes include [Zn(NH₃)₂X₂] (X = Cl,Br, I) [54] and [Ir(NH₃)Cl₅]²⁻ [55].

1.1.4. Linear Chain Ammine Complexes

Mixed-valence compounds such as $Pd^{II}Pt^{IV}(NH_3)_4Cl_6$ and $Pd^{II}Pd^{IV}(NH_3)_4Cl_6$ take the form of a chain structure as shown below:

$\bigcirc = N$

$\bullet = Cl$
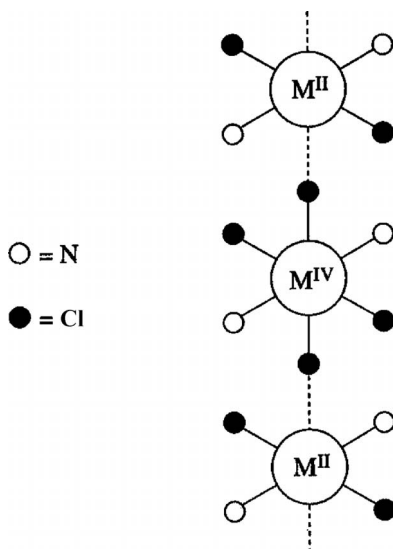
Both compounds exhibit an intense, extremely broad electronic absorption band in the visible region. The IR spectra of these mixed-valence compounds are approximately superpositions of those of each of the components. However, the RR spectra (Secs. 1.22 and 1.23 of Part A) obtained by using exciting lines in this
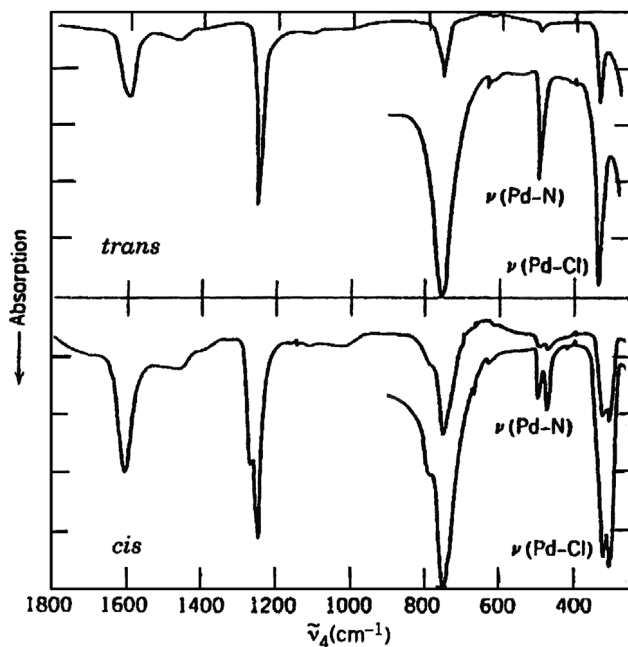

Fig. 1.5. Infrared spectra of trans- and cis-[Pd(NH3)2Cl2] [51].

region are markedly different from the IR spectra. In the case of the Pd−Pt complex, RR spectra involving the progressions of three totally symmetric metal–chlorine stretching vibrations were observed. Thus, the visible spectrum was attributed to a metal–metal mixed-valence transition. On the other hand, the Pd−Pd complex exhibits a RR spectrum involving several stretching and bending fundamentals and their combinations and overtones that originate in the Pd $(NH_3)_2Cl_4$ component only. Thus, Clark and Trumble [56] attributed the visible spectrum to the metal–ligand charge transfer transitions within this component. Later, this work was extended to the Ni−Pt complex of ethylenediamine (Sec. 1.2.3).

In the Magnus green salt, $[Pt(NH_3)_4] [PtCl_4]$, the Pt(II) atoms form a linear chain structure with relatively short Pt−Pt distances ($\sim$3.3 Å). Originally, Hiraishi et al. [13] assigned the infrared band at $200 \, cm^{-1}$ to a lattice mode that corresponds to the stretching mode of the Pt−Pt−Pt chain. This high frequency was justified on the basis of the strong Pt−Pt interaction in this salt. Adams and Hall [57], on the other hand, assigned this mode at $81 \, cm^{-1}$, and the $201 \, cm^{-1}$ band to a NH_3 torsion. In fact, the latter is shifted to $158 \, cm^{-1}$ by the deuteration of NH_3 ligands [58]. Different from the mixed-valence complexes, the Raman spectrum of the Magnus green salt obtained by excitation in the visible absorption band does not display long overtone series [58]. This is expected since it has no axial bonds that would change the bond lengths on electronic excitation. Resonance Raman spectra of these and other linear chain complexes are reviewed by Clark [59].

1.1.5. Lattice Vibrations of Ammine Complexes

Vibrational spectra of metal ammine complexes in the crystalline state exhibit lattice vibrations below $200 \, cm^{-1}$. Assignments of lattice modes have been made for the hexammine complexes of Mg(II),[2] Co(II) [60], Ni(II) [60,61], $[Co(NH_3)_6]/[Co(CN)_6]$ [62], and $[Pt(NH_3)_4]Cl_2$ [63]. Lattice modes and low-frequency internal modes of hexammine complexes have also been studied by Janik et al. [64,65] using the inelastic neutron-scattering technique.

1.1.6. Amido (NH₂) Complexes

The vibrational spectra of amido complexes may be interpreted in terms of the normal vibrations of a pyramidal ZXY_2-type molecule. Niwa et al. [66] carried out normal coordinate analysis on the $[Hg(NH_2)_2]_\infty^+$ ion (infinite-chain polymer); the results are given in Table 1.5. Brodersen and Becher [67] studied the infrared spectra of a number of compounds containing Hg−N bonds and assigned the HgN stretching bands at 700–$400 \, cm^{-1}$. Alkylamido complexes of the type $M(NR_2)_{4,5}$ (M = Ti,Zr,Hf,V,Nb,Ta) exhibit their MN stretching bands in the 700–$530 \, cm^{-1}$ region [68].

**TABLE 1.5. Infrared Frequencies and Band Assignments of Amido Complexes (cm^{-1}) [66]**

Compound	$v(NH_2)$	$\delta(NH_2)$	$\rho_w(NH_2)$	$\rho_r(NH_2)$	$v(HgN)$
$[Hg(NH_2)]_\infty^+ (Cl)_\infty^-$	3200 ⎫ 3175 ⎬	1540	1025	673	573
$[Hg(NH_2)]_\infty^+ (Br)_\infty^-$	3220 ⎫ 3180 ⎬	1525	1008	652	560

1.1.7. Amine(RNH_2) Complexes

Infrared spectra of methylamine complexes, $[Pt(CH_3NH_2)_2X_2]$ (X: a halogen), have been studied by Watt et al. [69]. Far-infrared spectra of $[M(R_2NH)_2X_2]$—[M = Zn(II) or Cd(II); R = ethyl or n-propyl; X = Cl or Br] type complexes have also been reported [70]. The $v(Pt-I)$ vibrations of $Pt(RNH_2)_2I_2$-type complexes are in the 200–150 cm^{-1} region [71]. Infrared and Raman spectra of metal complexes of aniline have been reviewed by Thornton [72].

1.1.8. Complexes of Hydrazine and Hydroxylamine

Hydrazine (H_2N-NH_2) coordinates to a metal as a unidentate or a bridging bidentate ligand. No chelating (bidentate) hydrazines are known. For example, the hydrazine ligands in $[M(N_2H_4)_2]Cl_2$ [M(II) = Mn,Fe,Co,Ni,Cu,Zn,Cd] are bridging bidentate (polymeric):
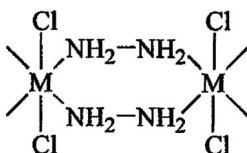
On the other hand, all hydrazine ligands in $[Co(N_2H_4)_6]Cl_2$ are coordinated to the Co atom as a unidentate ligand. According to Nicholls and Swindells [73], the complexes of the former type exhibit the $v(N-N)$ near 970 cm^{-1}, whereas those of the latter type show it near 930 cm^{-1}. The IR spectra of hydrazine complexes of M(II)(M = Ni,Co, Zn,Cd) [74], Os(II) [75], and Ln(III) (Ln = Pr,Nd,Sm) [76] have been reported. In these compounds, hydrazine acts as a unidentate or bridging bidentate ligand.

The vibrational spectra of hydroxyalmine(NH_2OH) have been reported by Kharitonov et al. [77]. Other related ligands include diazene (N_2H_2). Lehnert et al. [78] prepared a diazene-bridged Fe(II) dimer, $[FeL(PPr_3)_2]_2(\mu-N_2H_2)$, where L denotes 1,2-bis(2-mercaptophenylthio)ethane, and assigned the N_2H_2 vibrations on the basis of isotope shifths (H/D and $^{14}N/^{15}N$) and normal coordinate analysis. Andersen and Jensen [79] assigned the IR spectra of $M(I)_2[M(IV)L_2]$, where M(I) is an alkali metal ion; M(IV) is Ni, Fe, Mn, and V; and L is the $C_3H_6N_3O_3{}^{3-}$ ion (hexahydro-1,3,5-triazine-1,3,5-triol). Assignments were based on isotope shift data

(H/D, (^{14}N/^{15}N, ^{12}C/^{13}C, ^{58}Ni/^{62}Ni, and ^{54}Fe/^{57}Fe), and the IR spectrum of the free ligand, $C_3H_6N_3(OH)_3$.

1.2. COMPLEXES OF ETHYLENEDIAMINE AND RELATED LIGANDS

1.2.1. Chelating Ethylenediamine

When ethylenediamine(en) coordinates to a metal as a chelating ligand, it may take a *gauche* (δ and λ) or a *cis* conformation, as shown in Fig. 1.6. Then, eight different conformations are probable for the $[M(en)_3]^{n+}$ ion if we consider all possible combinations of conformations of the three chelate rings (δ or λ) around the chiral metal center. They are designated as $\Lambda(\delta\delta\delta)$, $\Lambda(\delta\delta\lambda)$, $\Lambda(\delta\lambda\lambda)$, $\Lambda(\lambda\lambda\lambda)$, $\Delta(\lambda\lambda\lambda)$, $\Delta(\lambda\lambda\delta)$, $\Delta(\lambda\delta\delta)$, and $\Delta(\delta\delta\delta)$. According to X-ray analysis, all the en ligands in the $[Co(en)_3]^{3+}$ ion take the *gauche* conformation (δ), and the configuration of the whole ion is $\Lambda(\delta\delta\delta)$ [80,81]. Although it is rather difficult to obtain such information from vibrational spectra, Cramer and Huneke [82] have shown that some of these conformers can be distinguished by the number of IR-active C−C stretching vibrations. For example, [Cr(en)$_3$]Cl$_3$ · 3.5H$_2$O [$\Lambda(\delta\delta\delta)$, $\mathbf{D}_3$ symmetry] exhibits only one band at $1003\,cm^{-1}$, whereas [Cr(en)$_3$][Ni(CN)$_5$] · 1.5H$_2$O [$\Lambda(\delta\delta\lambda$, $\delta\lambda\lambda)$, $\mathbf{C}_2$ symmetry] exhibits three bands at 1008, 1002 (shoulder), and $995\,cm^{-1}$. Gouteron has shown [83] that racemic (*dl*) and optically active (*d*) forms of [Co(en)$_3$]Cl$_3$ can be distinguished in the crystalline state by comparing vibrational spectra below $200\,cm^{-1}$.

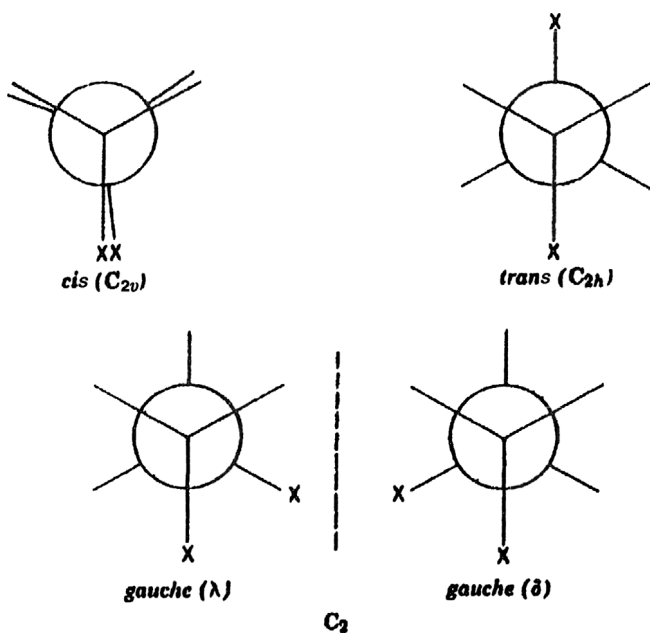**Fig. 1.6.** Rotational isomers of 1,2-disubstituted ethane. $X = NH_2$ for en.

Normal coordinate analyses on metal complexes of ethylenediamine have been made by several groups of workers. Fleming and Shepherd [84] carried out normal coordinate calculations on the 1:1(Cu/en) model of the $[Cu(en)_2]^{2+}$ ion. These workers considered a 9-atom system of C_{2v} symmetry, assuming that the two hydrogen atoms bonded to the C and N atoms are single atoms having the double mass of hydrogen. The IR bands at 410 and 360 cm^{-1} have been assigned to the ν(Cu−N) that are coupled with other skeletal modes. The corresponding Cu−N stretching force constant (GVF) was 1.25 mdyn/Å. Borch and coworkers [85–87] have carried out more complete calculations by considering all the 37 atoms of the $[Rh(en)_3]^{3+}$ ion ($[\Lambda(\delta\delta\delta)]$ configuration of D_3 symmetry), and the force constants (GVF) have been refined by using the vibrational frequencies obtained for the N–d_{12}, C–d_{12}, N,C–d_{24}, and their ^{15}N analogs. In total, 38 force constants were employed, including the Rh−N stretch of 1.607 mdyn/Å. Three ν(Rh−N) vibrations are at 545 (A_1), 445 (A_2), and 506 (E), although they are strongly coupled with other skeletal bending modes. Figure 1.7 shows the IR and Raman spectra of (N–d_{12}) [Rh(en)$_3$]Cl$_3$·D$_2$O obtained by Borch et al. [87]. Later, their calculations (E modes) were improved by Williamson et al. [88], who assigned the polarized Raman spectra of tris(ethylenediamine) complexes of Co(III) and Rh(III) on the basis of similar calculations.
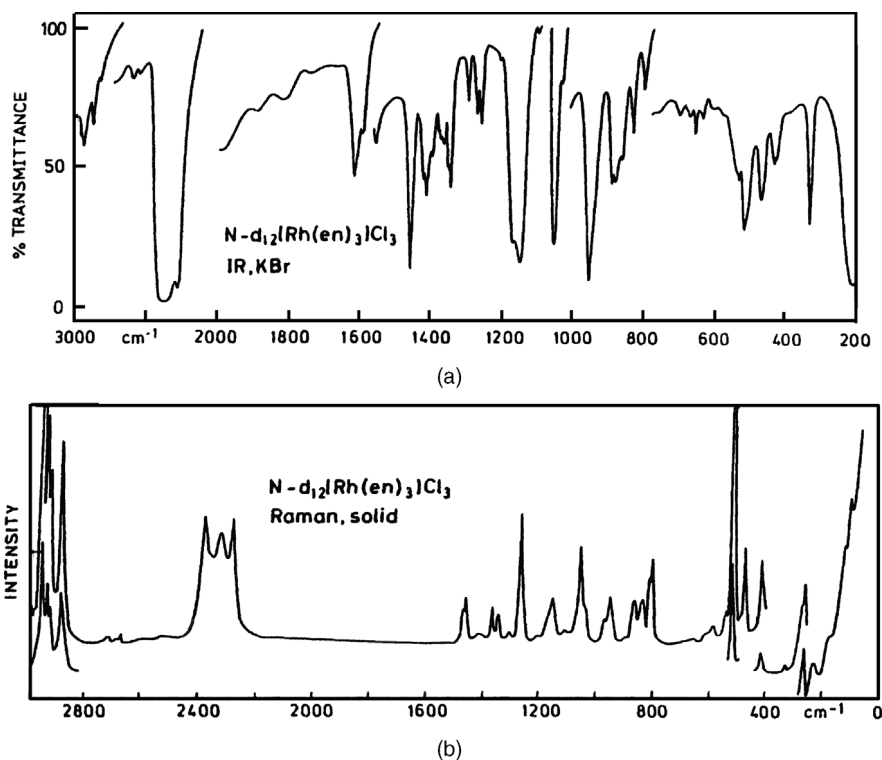

Fig. 1.7. Infrared (a) and Raman spectra (b) of N-deuterated (N-d_{12}) [Rh(en)$_3$]Cl$_3$·D$_2$O [87].

Empirical assignments of $v(M-N)$ have been reported for $[M(en)_3]^{3+}$ ($M = Cr, Co$) [89] $[M(en)_3]^{2+}$ ($M = Zn, Cd, Fe$, etc.) [90], and $[M(en)_2]^{2+}$ ($M = Cu, Pd, Pt$) [91]. Bennett et al. [92,93] found that, in a series of the $M(en)_3SO_4$ complexes, the $v(M-N)$ frequencies follow the order

$$
\begin{array}{cccccccccccc}
M = & \text{Mn(II)} & & \text{Fe(II)} & & \text{Co(II)} & & \text{Ni(II)} & & \text{Cu(II)} & & \text{Zn(II)} \\
v_4 & 391 & < & 397 & < & 402 & < & 410 & < & 485 & > & 405 \quad (\text{cm}^{-1}) \\
v_5 & 303 & < & 321 & \approx & 319 & < & 334 & < & 404 & > & 291
\end{array}
$$

As mentioned in Sec. 1.1.1, this is the order of stability constants known as the *Irving–Williams series*. These assignments have been confirmed by extensive isotope substitutions, including metal isotopes.

Stein et al. [94] observed that the Raman intensities of the totally symmetric stretching and chelate deformation modes of the $[Co(en)_3]^{3+}$ ion at 526 and 280 cm^{-1}, respectively, display minima near 21.5 kK,[*] where the d–d transition shows its absorption maximum. Figure 1.8 shows the excitation profiles of these totally symmetric vibrations, as well as that of non-totally symmetric $v(Co-N)$ (E_g) at 444 cm^{-1}. Since this result is opposite to what one expects from resonance Raman spectroscopy (Sec. 1.22 of Part A), it is called "antiresonance." These workers
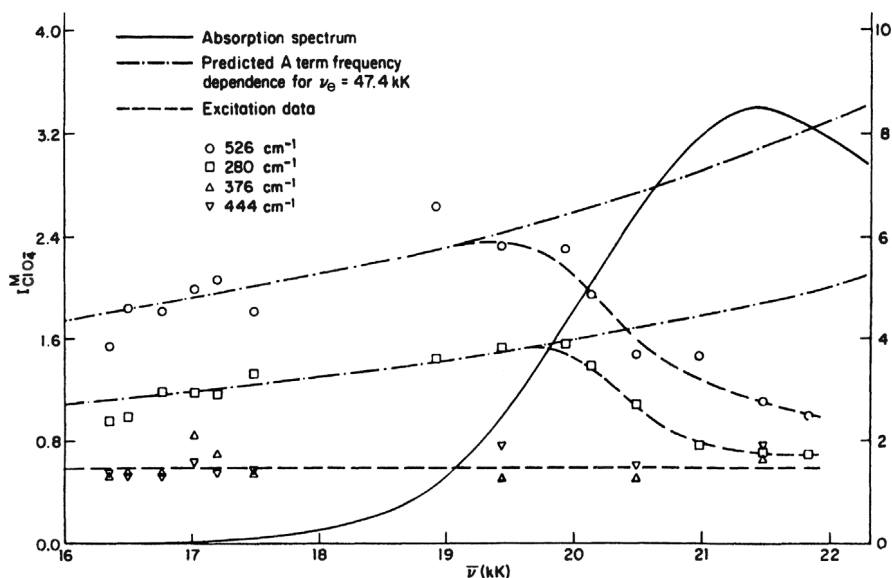
Fig. 1.8. *Excitation profiles for the $[Co(en)_3]^{3+}$ ion. The left-hand scale pertains to the excitation data and the right-hand scale, to the absorption spectrum. $I_{ClO_4^-}^M$ is the molar intensity relative to that of the v_1 band of ClO_4^-: $(I_{Co}/C_{Co})(C_{ClO_4^-}/I_{ClO_4^-})$. The theoretical curves ($-\cdot-\cdot-$) are calculated with the A term frequency dependence given by A. C. Albrecht and M. C. Hutley [J. Chem. Phys. **55**, 4438 (1971)].*

---

[*]1 kK = 1 kilokayser = 10^3 cm^{-1}.